

# The Formation of Pd Clusters Anchored to Grafted TiO<sub>2</sub>

*Highly dispersed Pd clusters on TiO<sub>2</sub> grafted SiO<sub>2</sub> (TiO<sub>2</sub>-SiO<sub>2</sub>) were prepared by impregnation with palladium(II) acetate solution followed by air calcination and hydrogen reduction. The structures of the grafted TiO<sub>2</sub> and the surface species formed on SiO<sub>2</sub> and TiO<sub>2</sub>-SiO<sub>2</sub> were characterized by X-ray absorption spectroscopy and FT-IR. XANES and EXAFS revealed that the grafted TiO<sub>2</sub> is isolated and each Ti atom is bonded to 4 oxygen atoms. Grafted TiO<sub>2</sub> promotes splitting of acetate ligands during impregnation and anchoring molecular palladium oxides on TiO<sub>2</sub>-SiO<sub>2</sub> through PdO<sub>x</sub> and TiO<sub>2</sub> interactions, leading to the formation of subnano Pd clusters. In contrast, Pd<sub>2</sub>O clusters aggregates on SiO<sub>2</sub> during air calcination, resulting in the formation of much larger Pd clusters. The average diameters of the clusters are about 7 Å for Pd/TiO<sub>2</sub>-SiO<sub>2</sub> and 20 Å for Pd/SiO<sub>2</sub>.*

The interactions between noble-metal clusters and non-reducible-metal-oxide carriers are critically important in determining the properties of materials used in catalysts and sensors. The properties of those materials can be further modified and enhanced by addition of a small amount of a second metal oxide. The role of the second metal oxide in changing the catalytic performance is poorly understood because of the lack of structural information. In the present research, the formation of Pd clusters on TiO<sub>2</sub> grafted SiO<sub>2</sub> was explored by means of EXAFS spectroscopy. The results indicate that molecular PdO<sub>x</sub> is deposited and anchored onto the TiO<sub>2</sub> surface through strong PdO<sub>x</sub>-TiO<sub>2</sub> interactions. This new material is characterized by highly thermal stable PdO<sub>x</sub> clusters and high Pd dispersion, making it ideal for the use as a catalyst and sensor. This study is expected to gain insights in how the second metal oxide on the catalyst support influences the structure and properties of the related materials.

Palladium is the metal of choice because it is widely employed as an active component for catalytic reactions and gas sensors. Palladium(II) acetate was chosen as the Pd precursor because the associated acetate ligand makes it possible to adopt vibrational and X-ray absorption spectroscopies for structural characterization. These techniques help to characterize the surface species formed on the carrier. Silica and TiO<sub>2</sub> were chosen as the support (or carrier) and the second metal oxide, respectively. The strong interaction between TiO<sub>2</sub> and metal has attracted a great attention in the last two decades due to its enhancement of catalytic properties. In addition, silica possesses high surface area and higher resistance than TiO<sub>2</sub> towards sintering at high temperature, allowing the TiO<sub>2</sub> grafted silica to exhibit high TiO<sub>2</sub> coverage and be a better support than TiO<sub>2</sub> alone. Higher dose of Pd precursor and, in turn, Pd clusters can be expected to bond to TiO<sub>2</sub> on this support. High signal to noise ratio in the EXAFS data of Pd can be obtained and thus minimizes the

influence of noise on the accuracy of Pd-TiO<sub>2</sub> characterization.

Some important structural information can be obtained from the Fourier transform of the EXAFS functions, even without detailed quantitative analysis. Fig. 1 shows the Ti-O phase-corrected Fourier transform characterizing Ti(OCH(CH<sub>3</sub>)<sub>2</sub>)<sub>4</sub> and TiO<sub>2</sub>-SiO<sub>2</sub> at the Ti K-edge. As for the Ti(OCH(CH<sub>3</sub>)<sub>2</sub>)<sub>4</sub> sample, the peak at a distance of about 1.8 Å and the peak located between 2.8 and 4.0 Å are contributions from Ti-O and Ti-C scattering. During the impregnation, the H-bonded hydroxyl groups on the SiO<sub>2</sub> surface react with isopropoxide ligands, hence, diminish the amplitude of the peak located between 2.8 and 4.0 Å and shift the peak at a distance of about 1.8 to 1.9 Å. After the calcination of adsorbed Ti(OCH(CH<sub>3</sub>)<sub>2</sub>)<sub>4</sub> on SiO<sub>2</sub>, the amplitude of the peak at 1.9 Å increased and one more peak appeared at about 2.7 Å, suggesting the presence of interactions between SiO<sub>2</sub> and TiO<sub>2</sub>.

A pre-edge peak at 4969.37 eV was observed in XANES spectra for the TiO<sub>2</sub>-SiO<sub>2</sub> sample. This feature is attributed to a 1s-3d transition, which is mainly caused by mixing of the 2p orbital with the 3d π-orbital of the Ti atom. Inferred from the correlation between pre-edge peak energy for Ti model compounds and their coordination geometry reported in the literature, Ti atom is suggested to be predominantly 4-fold coordinated. This is consistent with our EXAFS results. As shown in Fig. 1, the amplitude of the peak characterizing Ti-O contribution for TiO<sub>2</sub>-SiO<sub>2</sub> sample was slightly less than that for Ti(OCH(CH<sub>3</sub>)<sub>2</sub>)<sub>4</sub>. Detailed EXAFS data analysis showed that the average distances of Ti-O and Ti-Si are 1.90 and 2.87 Å, respectively, and the average coordination numbers are 3.7 and 1.6, indicating that isolated TiO<sub>4</sub> units dominate on the silica surface.

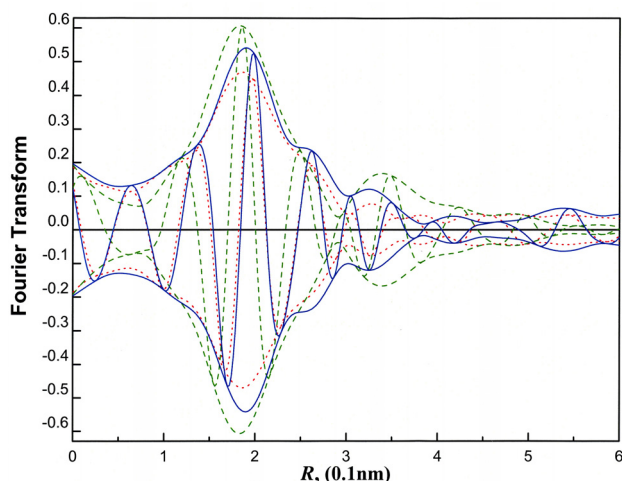


**Fig. 1:** Magnitude and imaginary parts of the EXAFS Fourier transform ( $3.5 < k < 10.0 \text{ \AA}^{-1}$ , Ti-O phase corrected) for  $\text{Ti}(\text{OCH}(\text{CH}_3)_2)_4$  (green dash line),  $\text{Ti}(\text{OCH}(\text{CH}_3)_2)_4$  adsorbed on  $\text{SiO}_2$  (red dotted line), and  $\text{TiO}_2\text{-SiO}_2$  (blue solid line).

Figure 2 shows the Pd-Pd phase and amplitude corrected Fourier transformed EXAFS functions for hydrogen-reduced  $\text{Pd}/\text{TiO}_2\text{-SiO}_2$  and  $\text{Pd}/\text{SiO}_2$  samples. The peak corresponding to the first Pd-Pd shell (at about  $2.7 \text{ \AA}$ ) for the  $\text{Pd}/\text{SiO}_2$  sample is much higher than that for  $\text{Pd}/\text{TiO}_2\text{-SiO}_2$ . Since the intensity of the Fourier transformed EXAFS function is proportional to the coordination number, this result indicates that  $\text{Pd}/\text{SiO}_2$  has much larger Pd cluster size. Detailed analysis of the EXAFS data confirmed this result. The coordination number of the first Pd-Pd shell is 4.1 and 8.8 for  $\text{Pd}/\text{TiO}_2\text{-SiO}_2$  and  $\text{Pd}/\text{SiO}_2$ , respectively. Moreover, the Fourier transforms indicate the presence of smaller peaks at approximately  $3.8$ ,  $4.8$ , and  $5.4 \text{ \AA}$  for  $\text{Pd}/\text{SiO}_2$ . These distances are consistent with the second, third, and fourth shell of bulk fcc Pd, indicating that Pd clusters on  $\text{SiO}_2$  are present in a state similar to that of the bulk metal. The high Pd-Pd shell contributions are hardly to be found on  $\text{Pd}/\text{TiO}_2\text{-SiO}_2$  because of the rather small Pd clusters. If a fcc structure is assumed for the Pd clusters and the ratio of the coordination number of Pd-O<sub>s</sub> to that of Pd-Pd ( $N_{\text{Pd-O}_s}/N_{\text{Pd-Pd}}$ ) is taken into account, these Pd-Pd first shell coordination numbers translate to diameters of approximate  $7$  and  $20 \text{ \AA}$  for  $\text{Pd}/\text{TiO}_2\text{-SiO}_2$  and  $\text{Pd}/\text{SiO}_2$ , respectively.

For the  $\text{Pd}/\text{TiO}_2\text{-SiO}_2$  sample, two smaller peaks appeared at  $1.7$  and  $3.5 \text{ \AA}$ . These two peaks are the characteristic peaks for metal-support interactions. As comparing the amplitude function derived from these two peaks with that obtained from theoretical calculation, the peaks at  $1.7$  and  $3.5 \text{ \AA}$  are inferred to be contributions from Pd-O and Pd-Ti. Detailed analysis showed that the average coordination number and bond distance are  $0.7$  and  $2.07 \text{ \AA}$  for Pd-O, and  $0.6$  and  $3.62 \text{ \AA}$  for Pd-Ti. The M-O distance in the range of  $2.0\text{-}2.2 \text{ \AA}$  suggests

the characteristic of the metal-oxygen bonding in supported metals without hydrogen adsorbed at the metal-support interface. The Pd-O distance of  $2.07 \text{ \AA}$  is in agreement with this indication.

The structural information of Pd-Ti interactions on  $\text{TiO}_2$ -supported Pd catalysts has not been reported in the literature. The Pd clusters prepared by the method reported here is rather small. Hence, a large fraction of atoms bonded to Pd would be contributed from the grafted  $\text{TiO}_2$ , yielding an EXAFS function with signal-to-noise level high enough for data analysis.

The EXAFS data for unreduced  $\text{PdO}_x/\text{TiO}_2\text{-SiO}_2$  and  $\text{PdO}_x/\text{SiO}_2$  samples are shown in Fig. 3. After Pd-Pd phase-corrected Fourier transformation, a peak appeared at about  $3.1 \text{ \AA}$  for the  $\text{PdO}_x/\text{SiO}_2$  sample. The results suggest the aggregation of palladium oxide leading to a formation of  $\text{PdO}_x$  clusters on  $\text{SiO}_2$ . In contrast, after calcination, two small peaks appeared in the region between  $2.5$  and  $4.0 \text{ \AA}$  for the  $\text{PdO}_x/\text{TiO}_2\text{-SiO}_2$  sample. Detailed EXAFS analysis showed that the  $\text{PdO}_x/\text{SiO}_2$  sample has an average Pd-O bond distance of  $2.02 \text{ \AA}$  and Pd-Pd bond distance of  $3.12 \text{ \AA}$ . Comparing the crystallographic data of  $\text{PdO}_x$ , the distances are consistent with the first and second shell of  $\text{Pd}_2\text{O}$  (within  $0.2 \text{ \AA}$  deviations). Thus, we suggest that  $\text{Pd}_2\text{O}$  is formed concomitantly with aggregation on the  $\text{SiO}_2$  surface during air calcination. No aggregation of  $\text{PdO}_x$  was detected for  $\text{PdO}_x/\text{TiO}_2\text{-SiO}_2$  sample. Instead,  $\text{PdO}_x$  is anchored by the grafted  $\text{TiO}_2$ , as evidenced by the second shell of Pd-O<sub>s</sub> (where subscript *s* is noted as support oxygen) of  $2.0 \text{ \AA}$  average distance and Pd-Ti interaction of an average distance of  $3.6 \text{ \AA}$ .

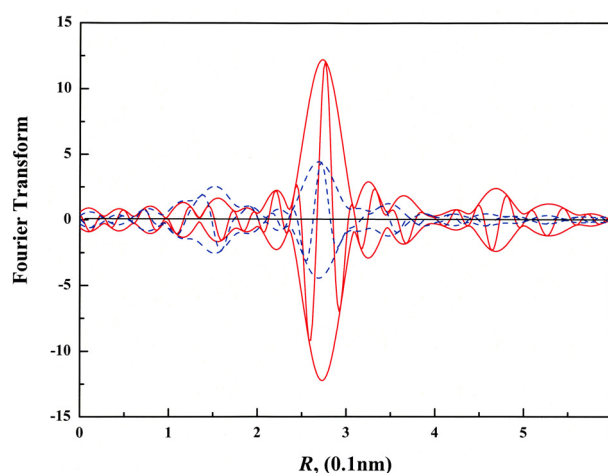


**Fig. 2:** Magnitude and imaginary parts of the EXAFS Fourier transform ( $4.0 < k < 13.0 \text{ \AA}^{-1}$ , Pd-Pd phase and amplitude corrected) for  $\text{PdO}_x/\text{TiO}_2\text{-SiO}_2$  (blue dotted line) and  $\text{PdO}_x/\text{SiO}_2$  (red solid line) both after  $200 \text{ }^\circ\text{C}$  reduction.

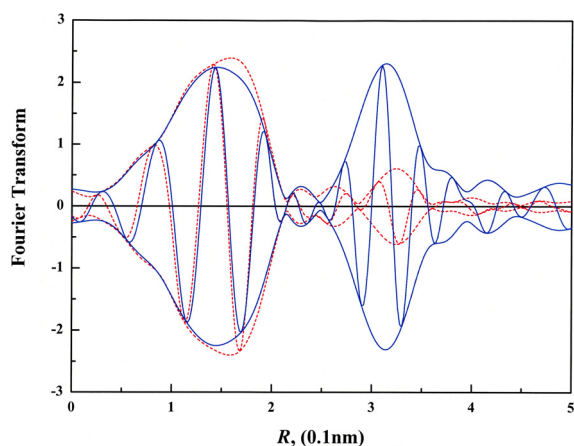


**Fig. 3:** Magnitude and imaginary parts of the EXAFS Fourier transform ( $4.0 < k < 13.0 \text{ \AA}^{-1}$ , Pd-Pd phase and amplitude corrected) for  $\text{PdO}_x/\text{TiO}_2\text{-SiO}_2$  (red dotted line) and  $\text{PdO}_x/\text{SiO}_2$  (blue solid line).

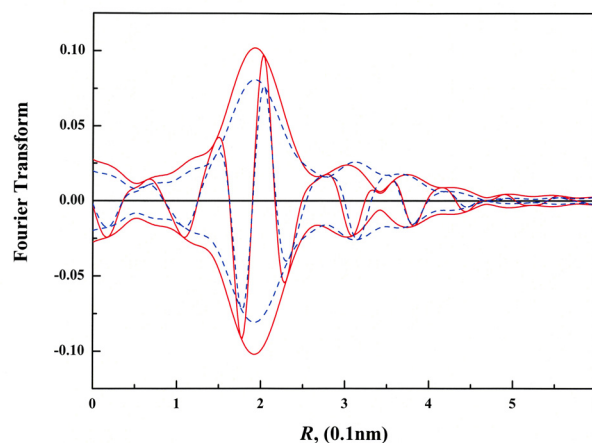


**Fig. 4:** Magnitude and imaginary parts of the EXAFS Fourier transform ( $4.0 < k < 10.0 \text{ \AA}^{-1}$ , Pd-O phase corrected) for  $\text{Ti}(\text{OCH}(\text{CH}_3)_2)_4$  adsorbed on  $\text{TiO}_2\text{-SiO}_2$  (blue dotted line) and  $\text{Ti}(\text{OCH}(\text{CH}_3)_2)_4$  adsorbed on  $\text{SiO}_2$  (red solid line).

Figure 4 displays a comparison of the  $k^1$ -weighted Pd-O phase corrected Fourier transforms for  $\text{Pd}(\text{Ac})_2/\text{TiO}_2\text{-SiO}_2$  and  $\text{Pd}(\text{Ac})_2/\text{SiO}_2$  samples. These results provide information about the interaction between  $\text{Pd}(\text{Ac})_2$  and the support. The amplitude of the peak at about  $2.0 \text{ \AA}$  for  $\text{Pd}(\text{Ac})_2/\text{SiO}_2$  is greater than that for  $\text{Pd}(\text{Ac})_2/\text{TiO}_2\text{-SiO}_2$ , while the amplitude of the peaks located between  $2.5$  and  $4.0 \text{ \AA}$  for  $\text{Pd}(\text{Ac})_2/\text{SiO}_2$  is lower. The peak at about  $2.0 \text{ \AA}$  is characteristic for Pd-O\* contribution, where O\* denotes the oxygen of acetate ligand. The lower amplitude of the peak for the  $\text{Pd}(\text{Ac})_2/\text{TiO}_2\text{-SiO}_2$  sample suggests that more  $\text{Pd}(\text{Ac})_2$  dissociates on the  $\text{TiO}_2\text{-SiO}_2$  support. The infrared data are in agreement with our conclusions. The characteristic infrared absorption band of acetic acid at  $892$  and  $1294 \text{ cm}^{-1}$  are observed for the  $\text{Pd}(\text{Ac})_2/\text{SiO}_2$  sample, whereas no significant absorption peaks are noticed for the  $\text{Pd}(\text{Ac})_2/\text{TiO}_2\text{-SiO}_2$  sample. The peaks in R-space between  $2.5$  and  $4.0 \text{ \AA}$  are contributed from the interaction of Pd with carbon of acetate ligands (Pd-C) and the interactions between Pd and the grafted  $\text{TiO}_2$ . The dissociation of  $\text{Pd}(\text{Ac})_2$  on  $\text{TiO}_2\text{-SiO}_2$  would result in a decrease of amplitude of the characteristic peaks of Pd-C. Therefore, a lower amplitude would be expected for the peaks located between  $2.5$  and  $4.0 \text{ \AA}$ . Yet, the opposite outcome was observed in the experimental data. The results thus suggest the existence of interactions between Pd and the grafted  $\text{TiO}_2$ . Based on the EXAFS results, we conclude that the grafted  $\text{TiO}_2$  helps to anchor  $\text{Pd}(\text{Ac})_2$  and prevents the agglomeration of  $\text{PdO}_x$  during calcination thereby enhancing the Pd dispersion on the  $\text{TiO}_2\text{-SiO}_2$  support.

#### BEAMLINE

01C1 SWLS/EXAFS beamline  
17C1 W20/EXAFS beamline

#### EXPERIMENTAL STATION

EXAFS end station

#### AUTHORS

J.-R. Chang  
Center for Nano-technology Design & Prototyping,  
National Chung Cheng University, Chia-Yi, Taiwan  
S.-G. Shyu  
Institute of Chemistry, Academia Sinica, Taipei, Taiwan  
J.-F. Lee  
National Synchrotron Radiation Research Center,  
Hsinchu, Taiwan

#### PUBLICATIONS

- C.-C. Shih and J.-R. Chang, *Mater. Chem. Phys.*, **92**, 89 (2005).
- W.-B. Su, M.-T. Tang, and J.-R. Chang, *Ind. Eng. Chem. Res.*, **44**, 1677 (2005).
- H.-M. Lin, S.-T. Kao, K.-M. Lin, J.-R. Chang, and S.-G. Shyu, *J. Catal.*, **224**, 156 (2004).

#### CONTACT E-MAIL

chmjrc@ccunix.ccu.edu.tw